Semicond. Sci. Technol. 9 (1994) 2073–2079. Printed in the UK

Optical characterization of pure ZnSe epilayers grown by metal organic vapour-phase epitaxy

A Chergui†, J Valenta†§, J L Loison†, M Robino†, I Pelant†§, J B Grun†, R Levy†, O Briot‡ and R L Aulombard‡

† Institut de Physique et Chimie des Matériaux de Strasbourg, Groupe d'Optique Nonlinéaire et d'Optoélectronique, Unité Mixte 380046, CNRS-ULP-EHICS 23, rue du Loess, BP 20 CR, 67037 Strasbourg Cedex, France
‡ Université de Montpellier II, Groupe d'Études des Semi-conducteurs, URA 357 de CNRS, BP 21 place Eugène Bataillon, 34095 Montpellier Cedex 5, France

Received 28 April 1994, in final form 15 August 1994, accepted for publication 25 August 1994

Abstract. Different ZnSe/GaAs epilayers prepared by low-pressure metal organic vapour-phase epitaxy under the conditions given by Nurmikko and Gunshor (1993 *Physica* B **185** 16) are studied through their low-temperature transmission, reflection and photoluminescence spectra. Several samples are etched out from their GaAs substrate and the properties of as-grown surfaces and etched surfaces are compared. The etched samples seem to be free of in-plane strain and to behave like bulk ZnSe. The free-exciton excited state ($n = 2$) is clearly observed in transmission, reflection and luminescence spectra. We also studied the thermal quenching of the photoluminescence in order to confirm the origin of some bound-exciton centres.

1. Introduction

Wide-bandgap II–VI semiconductors are promising materials for visible-light-emitting diodes, lasers or devices for nonlinear optics applications [1]. Among them ZnSe, with an energy bandgap of 2.7 eV at room temperature (RT), has attracted the greatest interest. In the last few years several methods have been developed for epitaxial growth of high-quality ZnSe. In particular, molecular beam epitaxy (MBE) and metal organic vapour-phase epitaxy (MOVPE) can produce high-purity ZnSe layers on GaAs substrates even though there are always misfit dislocations and residual strain due to the lattice mismatch of about 0.27% (at RT). In addition, the thermal expansion coefficients of ZnSe and GaAs are different. Although some light-emitting diodes (LEDs) and diode lasers based on ZnSe have already been prepared which emit in the blue at RT [2], crucial problems remain to be solved: conductivity control, efficient p-doping and preparation of good electrical contacts.

The preparation of ZnSe epilayers has therefore still to be improved. This means that the characteristics of the samples have also to be measured with more precision and sensitivity. Among the different methods of characterization of semiconductors, however, linear optical spectroscopy remains one of the easiest and most sensitive methods to obtain information on impurities, dislocations and strain in layers.

In this paper we study several MOVPE-grown samples of ZnSe epilayers by measuring their transmission, reflection and photoluminescence (PL) spectra. We also remove the GaAs substrates from the ZnSe epilayers and compare the optical properties of as-grown and etched surfaces.

We describe the sample preparation and the etching method in section 2 and the spectroscopic methods of characterization in section 3. The experimental results and their analysis are presented in section 4.

2. Sample preparation and etching

2.1. Sample growth

The samples described were grown on (001) GaAs substrates employing ASM-France OMR 12 MOVPE equipment [3]. We have H_2Se (5% in H_2) as the selenium precursor and either dimethyl zinc (DMZn) or triethylamine dimethyl zinc DMZn(NET3) as the zinc precursor (supplied by Epichem Ltd, UK) [3, 4]. The

§ Permanent address: Charles University, Faculty of Mathematics and Physics, Ke Karlovu 3, 121 16 Praha 2, Czech Republic.

0268-1242/94/112073+07$19.50 © 1994 IOP Publishing Ltd

Table 1. The growth parameters for the different ZnSe/GaAs epilayers discussed in the text: T_G denotes the growth temperature and d the thickness. The VI/II molar ratio and the growth pressure were kept the same, 5 and 40 Torr respectively. The ratios of the integrated intensities of the PL lines of free versus bound exciton lines (X/BX) and of free versus Y line (X/Y) are deduced from the PL experiments performed at 4.2 K (figures 1A and 1B), the label giving the number of the corresponding spectrum in figure 1.

Samples	Zn precursor	T_G (°C)	d (μm)	X/BX	X/Y	Label
ON7C	DMZn	500	5	2.92	2.64	1
ON7I	DMZn	500	1.3	0.304	4.28	2
ON6C	DMZn	320	5	0.033	9.42	3
ON6H	DMZn	320	1	0.255	362	4
93A11EF	TEADMZn	300	3	0.225	96.3	5

values of the growth parameters for the five samples studied in this paper are given in table 1. A detailed study of the optimization of the conditions of growth of these samples can be found in [3].

2.2. Etching procedure

The samples are typically of dimensions 6×4 mm^2. The ZnSe free epilayer surfaces are glued on glass slides by NOA61 Epotecny glue, their GaAs substrates then facing upwards.

The 0.5 mm thick GaAs substrates are first polished down to a thickness of 0.1 mm, first using different abrasive papers with SiC grains of decreasing size and finally a diamond polishing paste.

The remaining substrates are then totally removed by chemical etching. We proceed as follows: a jet of NH_4OH:H_2O_2 (1:20) solution is directed onto the GaAs surface of the sample, tightly fixed to a plastic lattice. Therefore, the jet, after having chemically etched the substrate, removes the by-products of the etching from the sample. If we keep on directing the jet onto the sample, one begins to etch the ZnSe layer itself but at a much slower rate (0.1 μm min^{-1}) than the GaAs substrate (2 μm min^{-1}). We were therefore able to remove that part of the sample which was in close contact with the GaAs substrate and contains more dislocations and impurities (As, Ga).

3. Experimental results and discussion

3.1. Spectroscopic set-up

Transmission and reflection experiments were performed using the broad spectral emission of a 50 W tungsten lamp. Its radiation was spatially filtered by two diaphragms and focused onto the sample placed inside a cryostat. PL was excited by an HBO 100 W high-pressure mercury lamp, the light of which was spectrally filtered through a 365 nm (3.40 eV) interference filter.

The transmission was measured in a straight configuration while the reflection and the PL were performed in a 60° or 90° configuration. The reflected, transmitted or emitted light was dispersed in a 0.65 m grating monochromator and detected by a photomultiplier tube (S20 photocathode). For sample cooling, we used two types of cryostat: a helium-bath glass cryostat (for liquid-He temperature, 4.2 K, and pumped liquid-He temperature, 2 K) and a He gas-flow cryostat (5–300 K).

3.2. Experimental results

We performed PL and reflectivity measurements in the near-band-edge region of each sample and transmission measurements for samples released from their substrates by selective etching.

The near-band-edge luminescence spectra for five different samples are compared in figure 1. One can clearly see in figure 1A that the spectra are dominated by free-exciton (denoted X in the figures), neutral donor-exciton complex (I_2), ionized donor–exciton complex (I_3) and acceptor–exciton complex (I_1) recombination lines. Weak emission lines are found at lower photon energies (figure 1B). They are two-electron satellites (TES) of some donors, donor–acceptor pair (DAP) radiative recombination lines and several further deep-level lines, namely the so-called Y-line (2.6 eV) associated with intrinsic defects and the S-line (with its LO-phonon replicas) representing a DAP luminescence involving a shallow donor and a deep acceptor. All the lines have been assigned according to their spectral positions [5].

Furthermore, it will be noticed that, despite similar near-band-edge luminescence spectra, the samples can have very different luminescence spectra at still lower photon energies due to donor–acceptor pair radiative recombination as shown in [5] for instance. Samples 1 and 2 emit a very intense DAP yellow luminescence, which indicates a very high impurity content and a poor device quality. The other samples present mainly blue near-band-edge luminescence spectra and are of a much better quality.

ZnSe (T_d point group symmetry) possesses a topmost fourfold degenerate valence band (with its maximum at the zone centre having a Γ_8 symmetry ($J = 3/2$)). In ZnSe films grown on (100)-oriented GaAs, an in-plane biaxial strain induced by the lattice mismatch of 0.27% at RT between ZnSe and GaAs and an in-plane

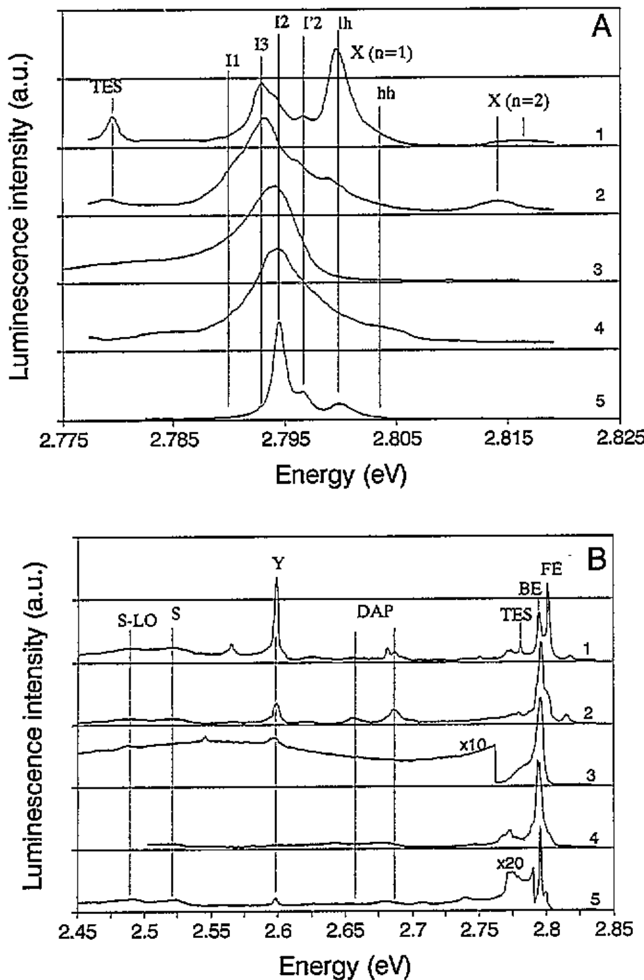

Figure 1. Normalized photoluminescence (PL) spectra of the five different ZnSe epilayers (growth parameters given in table 1) at liquid-He temperature (4.2 K), excited by the 365 nm emission of a HBO 100 W mercury lamp.

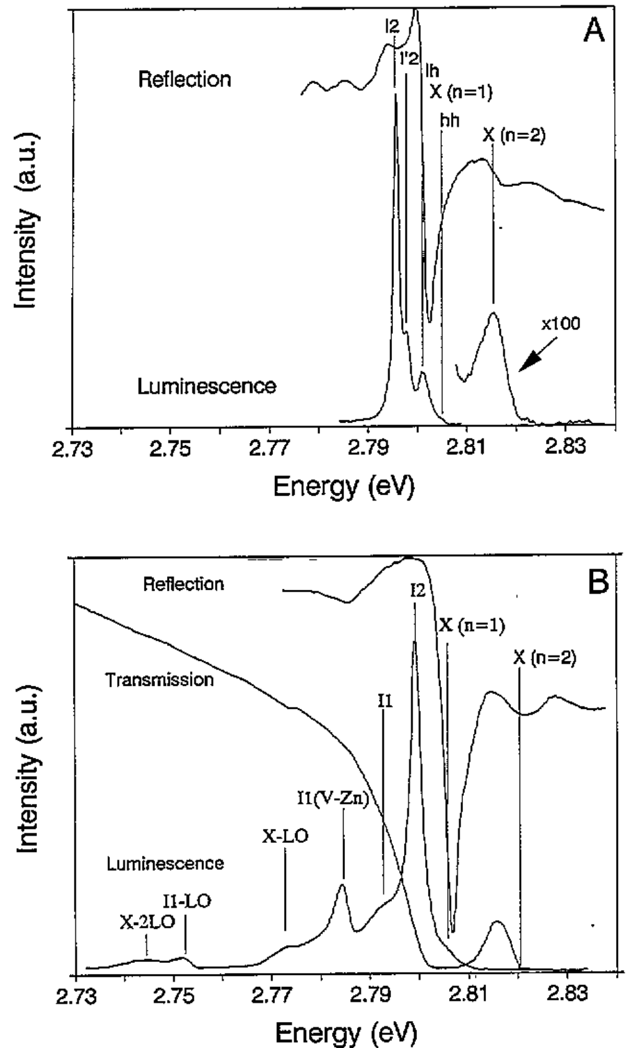

Figure 2. Comparison of the photoluminescence, reflection and transmission obtained on the as-prepared (A) or the etched (B) surface of the ZnSe epilayer (sample 5) released from the GaAs substrate.

tensile strain induced by the different thermal expansion coefficients of the epilayer (6.8×10^{-6} K at RT) and the substrate (5.8×10^{-6} K at RT) [6] remove the degeneracy of the topmost valence band. This band splits into two doubly degenerate subbands (the so-called 'heavy-hole' band (hh, $m_J = \pm 3/2$) and the 'light-hole' band (lh, $m_J = \pm 1/2$)). As a consequence, two types of excitons can be formed from electrons in the lowest conduction band ($J = 1/2$, Γ_6 symmetry) and either light holes or heavy holes [7]. It is well understood now [8, 9] that an epilayer grows coherently on its substrate in the early stage, until a 'critical' layer thickness (0.15 μm) is reached. Then misfit dislocations release the strain in the layer. Therefore in our samples, which have a thickness of about 1 μm after growth, only the tensile thermally induced strain should remain. Indeed, the splitting of the X and I_2 lines into doublets can be clearly seen in spectra 1 and 5 of figure 1A: X_{hh} is centred at about 2.803 eV while X_{lh} is at 2.800 eV, for instance.

The selective etching of GaAs substrates enables us to compare the optical characteristics (PL and reflection) of free surfaces of as-grown samples with those of etched surfaces of samples once released from their GaAs substrate. In this case we also measured their transmission spectra. In figures 2 and 3 we compare samples with the most pronounced excitonic structure. In etched samples the lh–hh splitting of the emission lines disappears and the free-exciton line becomes relatively weak. Besides this, all emission lines are remarkably blue-shifted and a new emission line is observed at 2.784 eV. The appearance of an emission line at this spectral position and its increase at the expense of the free exciton emission have been previously explained by excitons bound to Zn vacancies [5]. This explanation could still be correct for the etched surfaces of our samples, where Zn vacancies could be a consequence of their former proximity to the GaAs substrate. The hypothesis of excitons bound to arsenic atoms, which have diffused from the substrate, can be disregarded due to the difference of about 7 meV between the binding energy of the exciton to this centre [10] and the corresponding value deduced from the spectral position of this line.

I_2 lines are often interpreted in the literature as being due to excitons bound to Ga donors or In, Cl donors. In our spectra we found no noticeable increase of I_2 lines

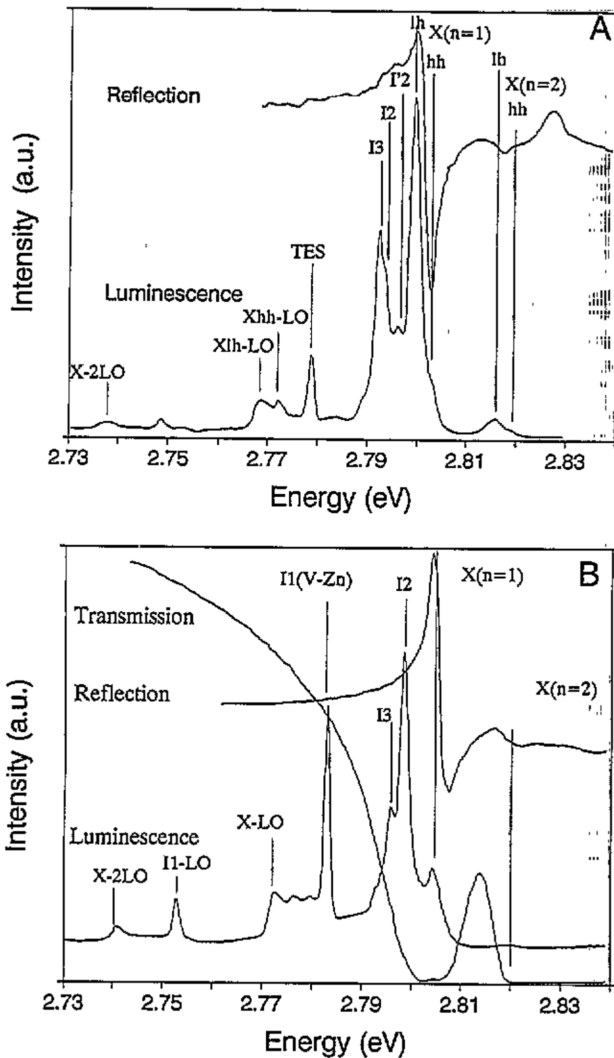

Figure 3. As figure 2 but for another epilayer (sample 1).

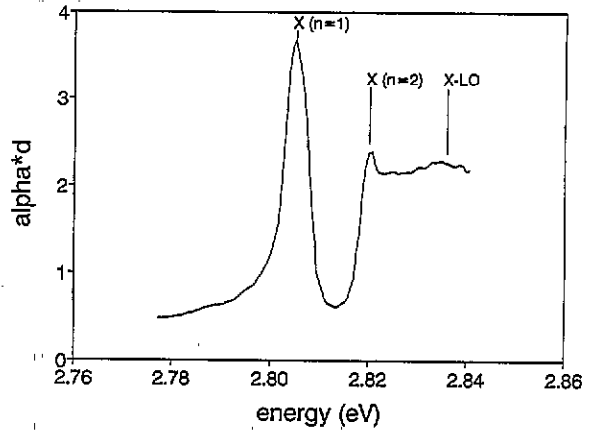

Figure 4. Absorption spectrum of sample 5, thinned to about 0.5 μm by chemical etching, at 2 K.

on etched surfaces when compared with as-grown ones, as would have been expected for excitons bound to Ga donor centres. This supports the interpretation of the I_2 line [11] as being due to excitons bound to neutral donors which originate from the precursors (In or Cl).

The PL spectra of etched samples are nearly identical to those of bulk ZnSe and ZnSe homoepitaxial layers [11, 12]. Therefore, we can deduce that both mismatch strain and thermally induced strain are almost relaxed when the GaAs substrate has been removed. In this context we note that the reflection spectra are very helpful in determining the spectral positions of free-exciton transitions. On the other hand, the transmission spectra reflect the excitonic absorption in the whole volume of the sample. To make the best use of transmission spectroscopy we need to have samples that are thin enough. For instance, as can be seen in figures 2 and 3, the transmission spectrum of a sample of about 2 μm thickness is saturated at the exciton resonance and in the absorption edge. The samples were further etched to a thickness of about 0.5 μm. Very interesting features could be observed in the transmission spectrum as can be seen in figure 4. Beside the first exciton line (1X) at 2.805 eV (FWHM = 6 meV), one can observe, on its high energy side, a narrower and weaker absorption line (2.820 eV) at an energy of 15 meV from the 1X resonance, and a broad absorption band (2.836 eV) at an energy of 31 meV above the 1X resonance. These two high-energy absorption structures have similar features in the luminescence and reflection spectra (see figures 2 and 3) [13].

The 2.820 eV line corresponds most probably to the $n = 2$ exciton state (2X). Therefore, from the spectral positions of the first two (1X and 2X) exciton lines, one can deduce the binding energy E_X^b of the exciton as well as the bandgap energy E_g, assuming a hydrogenic series of excitonic energies:

$$\hbar\omega_{nX} = E_g - \frac{E_X^b}{n^2} \qquad \text{with } n = 1, 2...$$

then

$$E_X^b = \tfrac{4}{3}(\hbar\omega_{2X} - \hbar\omega_{1X}) = 20 \text{ meV}$$

and

$$E_g = \tfrac{1}{3}(4\hbar\omega_{2X} - \hbar\omega_{1X}) = 2.825 \text{ eV}.$$

These values agree quite well with previously published results [14]. The theoretical 1/8 ratio of the oscillator strengths of the first two excitonic lines fits quite well with the experimental ratio deduced from the deconvolution of the experimental spectrum of figure 4.

Furthermore, we can see that the bandgap energy is on the low-energy side of the broad 2.836 eV absorption band. This band does not therefore directly belong to the exciton series. However, it could well be due to LO-phonon-assisted transitions towards the 1X exciton. These transitions have already been observed in polar semiconductors in absorption [15] but more often in PL and photoconductivity spectra [16, 17]. Because ZnSe has a polar character, LO-phonon-assisted transitions should be observable [18].

The 2X excitonic level has also been observed in reflection and in luminescence spectra (see figures 2 and 3). In figure 5 we compare, for instance, the exciton PL spectra of two of our samples normalized to the 1X luminescence line. One can see that the spectral shapes of the 1X and 2X emission lines are very similar. The

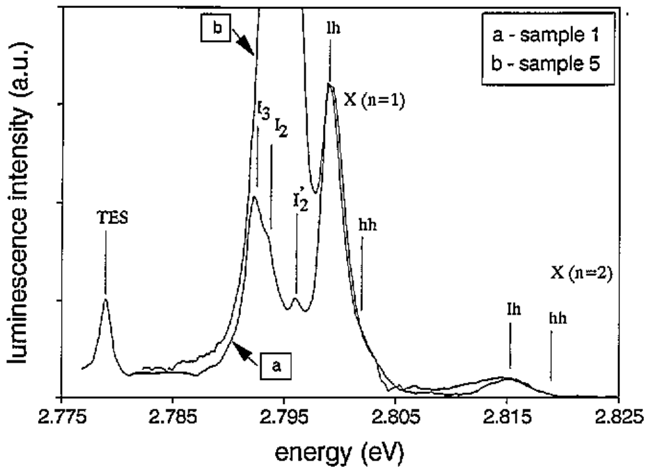

Figure 5. Details of the PL spectra ($T = 4.2$ K) of the two best ZnSe epilayers (samples 5 and 1). The free-exciton features $X(n = 1)$ and $X(n = 2)$ are almost identical, while the I_2 and I_2' lines (exciton bound to neutral donor) are much more intense for sample 5. (Note that, on the other hand, sample 1 possesses a significantly stronger Y line, see table 1.)

bound-exciton luminescence lines (I_1, I_2, I_3) have very different intensities.

This is the first time that the excitonic series has been so clearly observed in ZnSe epilayers deposited on GaAs substrates. Excited excitonic levels have been reported in several papers, but they were either the X_{lh} line in thin samples (0.17 μm in [14, 19]) or quite weak lines [3, 20, 21].

4. Thermal dependence of the luminescence

The temperature dependence of the luminescence of as-grown samples has also been measured in order to confirm the origin of some exciton lines and also to analyse the effect of strain on the PL.

Generally, when we increase the temperature of the samples, we observe a relative increase of the intensities of the free-exciton (X) lines compared with those of the bound-exciton lines (BX), due to the thermal dissociation of BX. A red shift of all lines is also noticed, which can be explained by bandgap shrinkage [22]. At temperatures above 40 K, all BX lines have completely disappeared.

Let us examine the temperature behaviour of the donor-bound exciton lines I_2 and I_2'. When we increase the temperature from 4 K to 40 K, the intensity of the I_2' line increases compared with the I_2 line (a1). Three possible interpretations of these two lines have been proposed. We will analyse them in the context of our experimental observations.

(i) They involve two different donor species (D_0, X) and (D_0', X). The disappearance of I_2 while I_2' is still there in etched samples could support this possibility. However, the I_2' should then decrease compared with the I_2 line, with increasing temperature. Indeed, the binding energy of the exciton for the I_2' line (D_0', X) (the difference in energy between I_2' and 1X lines) would be less than the binding energy of the exciton for the I_2 line (D_0, X) (the difference in energy between I_2 and 1X lines). Our observation is inconsistent with this hypothesis.

(ii) They are due to the ground and excited states of the same donor-bound exciton (D_0, X). The fact that the I_2' line disappears while the I_2 line remains when we remove the GaAs substrate, completely rules out this explanation.

(iii) The two I_2 and I_2' lines are due to the same donor-bound exciton level split by in-plane strain into lh and hh components as already shown in [4, 22, 23].

Two observations support this last interpretation. First, the fact that only one line, denoted I_2', remains is consistent with the strain relaxation expected after substrate removal. Second, the increase of the I_2'/I_2 ratio with increasing temperature corresponds to a thermal excitation of holes from the lh to hh valence bands, if the intensities of the I_2 and I_2' lines are proportional to the populations of the light and the heavy holes respectively. The equation $I_2'/I_2 = \exp(E_a/k_B T)$ holds, where E_a is the activation energy, which should be equal to the difference between the I_2' and I_2 lines [8]. This spectroscopic value is equal to 2 meV, independent of the temperature (figure 6). In order to find the thermodynamic activation energy from the preceding equation, we deconvolve the PL spectra into

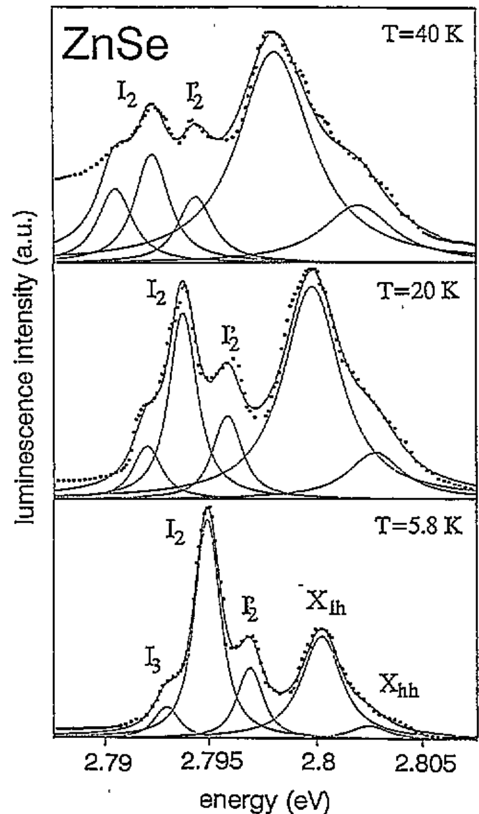

Figure 6. Three PL spectra of sample 5 taken at temperatures of 5.8, 20 and 40 K. The points are experimental; the dotted and full curves are the Voigt curves (results of the deconvolution of the experimental spectra) and their sum respectively.

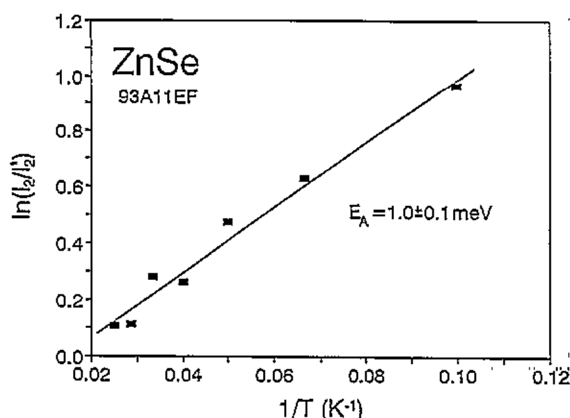

Figure 7. Arrhenius plot of the I_2/I_2' integral intensity ratio. The full line is the result of a linear regression. The 'thermodynamic' activation energy E_a is calculated from the slope of the line using the equation $I_2/I_2' = \exp(E_a/k_BT)$.

Voigt curves, in which the Gaussian width has been kept fixed (slit broadening) and the Lorentzian width has remained constant for all BX lines. Figure 6 shows three PL spectra taken at different temperatures in the excitonic region, along with their decompositions into Voigt curves. An Arrhenius plot of the I_2/I_2' integral intensity ratio then gives a linear dependence, yielding a thermodynamic activation energy $E_a = 1.0 \pm 0.1$ meV (figure 7). It differs therefore from the spectroscopic value of $E_a = 2$ meV, but this disagreement can at least partly be accounted for by a certain arbitrariness involved in the deconvolution procedure.

Another possible cause, which cannot be completely ruled out on the basis of our measurements, is that the I_2' line might be a superposition of the (D_0, X_{hh}) recombination with a weak BX line belonging to a different donor [24]. This could partly compensate for the decrease of I_2/I_2' with temperature, resulting in a lower effective thermodynamic value of E_a. We thus conclude that the I_2 and I_2' features in our samples are probably due to (D_0, X_{lh}) and (D_0, X_{hh}) radiative recombinations with possible interference of another donor.

Let us mention that, as in [4, 23, 25] and in contradiction to [22], the energy spacing of I_2 and I_2' (2 meV) is different from that of the free-exciton components $1X_{lh}$ and $1X_{hh}$ (about 3 meV) and increases with temperature (see figure 6). The overall 1X lineshape is also asymmetrical. These effects may be due to spatial dispersion and reabsorption near the polariton bottleneck [26]. The reflection near the exciton resonance has a spectral shape and a position (figures 2 and 3) that also reflects the influence of the polariton phenomenon [27].

5. Conclusions

We have studied a set of five samples of ZnSe epilayers deposited by MOVPE on monocrystalline substrates of GaAs. We made low-temperature measurements of their PL, reflectivity and transmission spectra. The samples that showed the most intense exciton luminescence had their GaAs substrates etched away. The optical characteristics of as-grown and etched surfaces were compared. We conclude that mismatch strain as well as thermally induced strain are almost released once the substrate is completely etched away. For the first time, the 2X exciton level has been clearly observed by PL, reflection and transmission measurements. The binding energy of the exciton is $E_X^b = 20 \pm 1$ meV.

The study of the temperature dependence of the two I_2 and I_2' emission lines in as-grown samples helps us to confirm that these lines are due to the radiative recombination of (D_0, X_{lh}) and (D_0, X_{hh}) donor-bound excitons with the possible superposition of the radiative recombination of another donor-bound exciton (D_0', X).

Acknowledgments

The authors would like to gratefully acknowledge fruitful discussions and a critical reading of the manuscript by B Hönerlage, and technical contributions concerning the etching procedure by G Schwalbach from the 'Institut de Physique et de Chimie des Matériaux de Strasbourg'.

One of the authors (JV) acknowledges the financial support of the European Union in the form of a TEMPUS individual mobility grant, no IMG-92-CS-1597. In addition, OB and RLA acknowledge a similar support in the form of an ESPRIT contract, no MTVLE6675.

References

[1] Nurmikko A V and Gunshor R L 1993 *Physica* B **185** 16
[2] Jeon H, Hagerott M, Ding J, Nurmikko A V, Grillo D C, Xie W, Kobayashi M and Gunshor R L 1993 *Opt. Lett.* **18** 125
[3] Cloitre T, Briot N, Briot O, Gil B and Aulombard R L 1993 *Mater. Sci. Eng.* B **21** 169
[4] Yao T, Okada Y, Matsui S, Ishida K and Fujimoto I 1990 *J. Crystal Growth* **81** 518
[5] Gutowski J, Presser N and Kudlek G 1990 *Phys. Status Solidi* a **120** 11
[6] Shibata N, Ohki A, Zembutsu S and Katsui A 1993 *Japan. J. Appl. Phys.* **27** L487
[7] Mohammed K, Cammack D A, Dalby R, Newbury P, Greenberg B L, Petruzzello J and Bhargava R N 1987 *Appl. Phys. Lett.* **50** 37
[8] Ohkawa K, Mitsuyu T and Yamazaki O 1988 *Phys. Rev.* B **38** 12465
[9] Saraie J, Matsumura N, Tsubokura M, Miyagawa K and Nakamura N 1989 *Japan. J. Appl. Phys.* **28** L108
[10] Yodo T and Yamashita K 1988 *Appl. Phys. Lett.* **53** 2403
[11] Blanconnier P, Hogrel J F, Jean-Louis A M and Sermage B J 1981 *Appl. Phys.* **52** 6895
[12] Tuchman J A, Kim S, Sui Z and Herman I P 1992 *Phys. Rev.* B **46** 13371
[13] Huang X M and Igaki K 1986 *J. Crystal Growth* **78** 24
[14] Madelung O (ed) 1982 *Landolt-Börnstein New Series* vol 17b (Berlin: Springer) p 126
[15] Ringeissen J, Coret A and Nikitine S 1968 *Localized Excitations in Solids* (New York: Plenum) p 297
[16] Weiher R L and Tait W C 1968 *Phys. Rev.* **166** 791
[17] Gross E F, Permagorov S A and Razbirin B S 1971 *Sov. Phys.–Usp.* **14** 104

[18] Miyazaki H and Hanamura E 1980 *Relaxation of Elementary Excitations* (Berlin: Springer) p 71
[19] Yao T, Takeda T and Watanuki R 1986 *Appl. Phys. Lett.* **48** 1615
[20] Ohki A, Shibata N and Zembutsu S 1988 *Japan. J. Appl. Phys.* **27** L909
[21] Shahzad K, Olego D J and Cammack D A 1989 *Phys. Rev.* B **39** 13016
[22] Shazad K 1988 *Phys. Rev.* B **38** 8309
[23] Potts J E, Cheng H, Mohapatra S and Smith T L 1987 *J. Appl. Phys.* **61** 333
[24] Kudlek G, Presser N, Pohl U W, Gutowski J, Lilja J, Kuusisto E, Imai K, Pessa M, Hingerl K and Sitter H 1992 *J. Crystal Growth* **117** 309
[25] Giapis K P and Jensen K F 1990 *J. Crystal Growth* **101** 111
[26] Sermage B and Voos M 1977 *Phys. Rev.* B **15** 3935
[27] Hopfield J J and Thomas D G 1963 *Phys. Rev.* **132** 563